DOI 10.52209/2706-977X_2025_3_8 **IRSTI 55.29.33** **UDC 621.7**

The Influence of Nonlinearity System of the Hydro-volume Vibration Mechanism on its Dynamic Characteristics

Moyzes B.*, Kuvshinov K., Plotnikova I., Vavilova G., Vtorushina A.
National Research Tomsk Polytechnic University, Tomsk, Russia
*corresponding author

Abstract. This work is the result of continuation of the research in the context of vibration parameters studying while the generation of an amplitude-frequency modulated signal of a shock-vibration seismic installation. The testing bench simulates the operation of the installation. There are two circuits – low-frequency and high-frequency oscillations in the testing bench. The article presents the results of research on separate operation of high-frequency and low-frequency generators. The main resonant frequencies during generators operation were determined in the study. These frequencies can be adjusted by changing the average pressure in the elastic shells. It is possible to reduce the nonlinearity of the vibration system of the experimental stand by increasing the average pressure in the hydraulic system. The system behaves in the same way with an insignificant difference in the resonant frequencies and amplitude values of the main resonant peak, with separate excitation of oscillations from high-frequency and low-frequency generators. The frequency of additional resonance is determined. This frequency is explained by several degrees of freedom of the vibration mechanism mechanical system. Possible modes of loading the system by oscillation generators are determined.

Keywords: vibration parameters, hydro-volume vibration mechanism, nonlinearity of the system, dynamic characteristics

Introduction

The issues of studying the parameters of vibration that accompanies the operation of various equipment [1-6] or is generated by technical systems [7-10] are always of great importance.

One of the areas of scientific research is vibration seismic exploration [11-15].

This research is a continuation of scientific articles [14, 15]. The purpose of the articles is to generalize the achieved results concerning the development of a shock-vibration source of seismic signals that generates an amplitude-frequency modulated signal.

It is proposed in the research [14] a design scheme of a seismic source with a vibration system and an impact mechanism. A hypothesis is put forward about the validity of replacing the fall of the load on its swinging-oscillatory motion in the research [15].

This motion is formed by the second oscillatory circuit, thus the hydro-volume mechanism consists of

- an oscillatory system with two circuits – low-frequency and high-frequency;
- a system for forming the initial pressure p_0;
- a load that presses the mechanism to the ground.

Experimental studies were first conducted with one generator – high-frequency, then – low-frequency.

The frequency change range is ω_1=0÷40 Hz and ω_2=0÷40 Hz.

The scheme for conducting experimental studies of dynamic characteristics is shown in Figure 1.

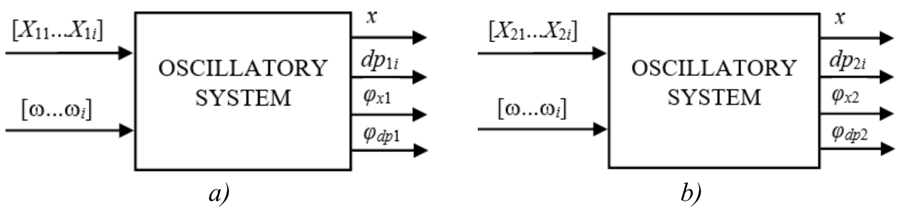

a) high-frequency; b*)* low-frequency x is the output signal; $dp_{1(2)}$ are the pressure drop; $\varphi_{x1(2)}$ and $\varphi_{dp1(2)}$ are the phase shift angles

Fig. 1. – The scheme of conducting of the experimental studies with excitation by generators:\

To analyze the obtained results, dependency diagrams were constructed (Fig. 2, 3):

- natural frequency ω_0 from the values of inputs $X_1$and X_2, and average pressure p_0;
- coefficient of the ratio of the resonant amplitude of oscillation x_{res} from the values of inputs X_1 and X_2

$$K_{res} = \frac{x_{res}}{X_{1(2)}}. \tag{1}$$

Modeling according to the system (2) [14], supplemented by formulas

$$V(t) = \frac{1}{m}\int_0^t dF(t)dt\,; \qquad (2)$$

$$x(t) = \int_0^t V(t)dt\,; \qquad (3)$$

was carried out with the initial pressure value p_0=1 MPa.

Let us recall [14] that the following notations are used in formulas (2, 3):

- *m* is the weight of the load;
- *V* is the movement speed of the movable body of the actuator;
- *x* is the current movement of the moving body.

The rationale for choosing the mean value will be studied in the next paper.

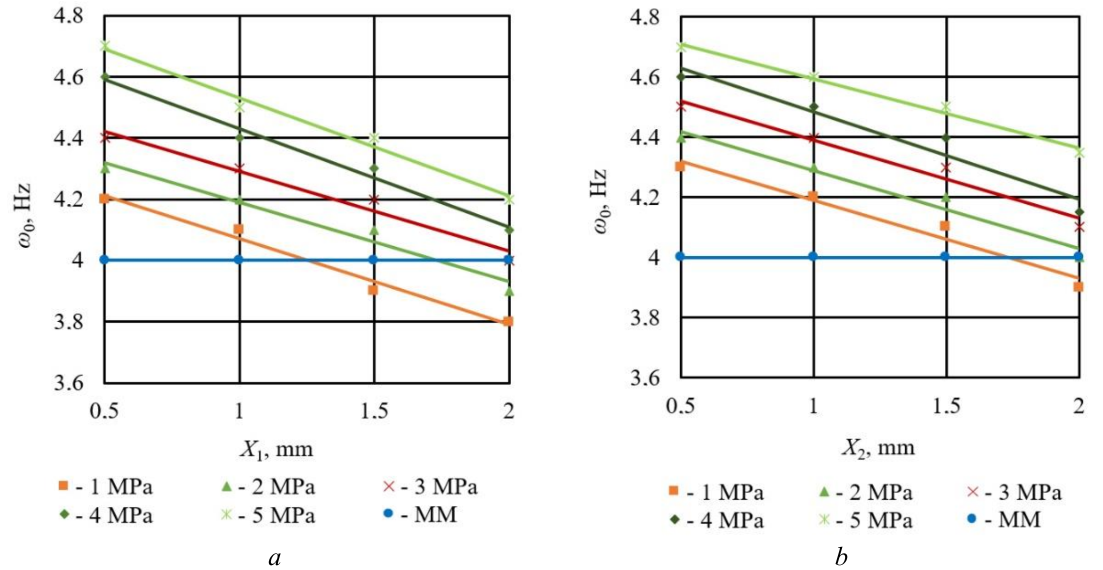

Fig. 2. – Dependences of the natural frequency ω_0 on the values of the average pressure p_0 and inputs and X_1 and X_2: *a* – X_1; *b* – X_2; MM – mathematical model

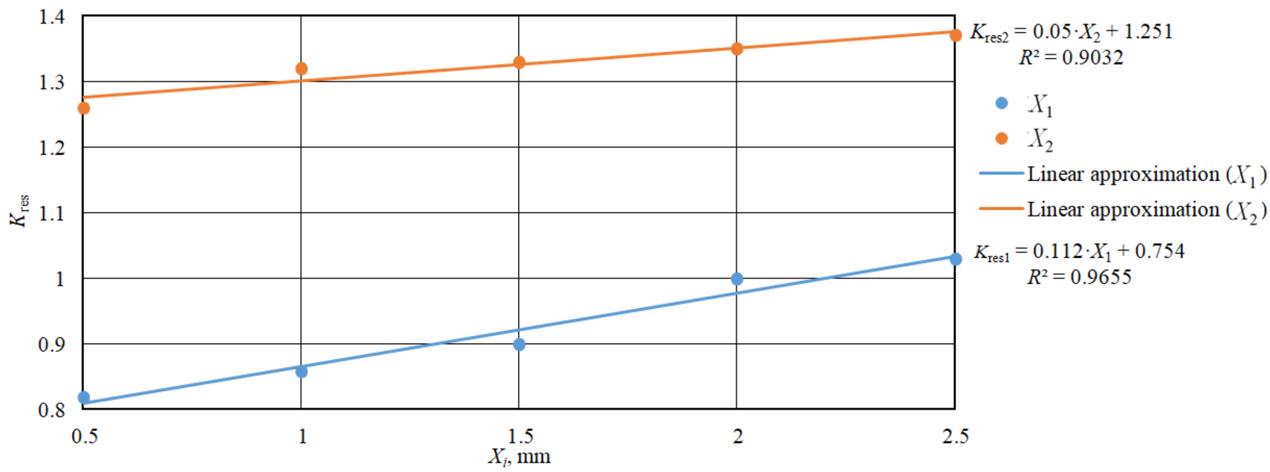

Fig. 3. – Dependence of the coefficient of the ratio of the resonant amplitude of oscillation K_{res} on the value of the inputs X_1 and X_2 at p_0=2 MPa

The results of the studies (Fig. 4, 5) [15] showed that the dynamic system of the vibration mechanism has (according to average values):

- the main resonance along the *x* coordinate and the pressure drop *dp* at the frequency

$$\omega_0 = \omega_x = \omega_{dp} \approx 4 \text{ Hz};$$

- additional resonance along the x coordinate

$$\omega_x' \approx 15.5 \text{ Hz};$$

- additional resonance along the pressure drop *dp*

$$\omega'_{dp} \approx 3.5 \text{ Hz}.$$

When comparing the obtained data (Fig. 4, 5) [15], we can conclude that:

• the obtained model, in the first approximation, describes the dynamic characteristics of the system relatively well;

• with different excitation options (from one or the other generator), there is a slight difference in the resonant frequencies of the first ω_{01} and second generators ω_{02}

$$\Delta\omega_0 = \omega_{0(X1)} - \omega_{0(X2)} \approx 0.1 \text{ Hz},$$

i.e. the oscillatory system of the vibration mechanism behaves almost identically when exposed to the generators.

At the same time, the linear model does not explain the presence of:

- additional resonance along the x coordinate at a frequency of ~15.5 Hz;
- a decrease in resonant frequencies with an increase in the $X_{1(2)}$ input (Fig. 2);
- a change in the value of the coefficients (Fig. 3).

1 Theoretical and Experimental Research

To assess the applicability of the developed linear mathematical model of the vibration mechanism, we will use the results of experimental studies [16-22]. It was found that a loop characteristic is observed between the change in volume dW and the pressure drop dp (Fig. 4, 5). This indicates the existing phase mismatch between dW and dp. Moreover, the direction of the loop indicates the accumulative properties of the shells.

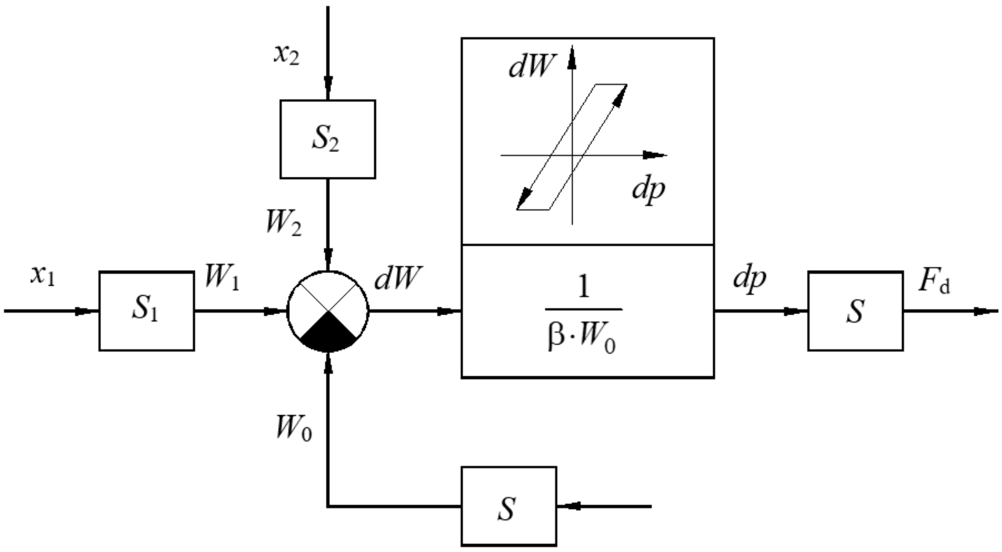

x_1, x_2 are the coordinates of the plungers moving; S_1, S_2 are the area of the generators plungers; S is the operating area of the actuator; $k_{S1}=S_1/S$ and $k_{S2}=S_2/S$ are the area ratio coefficients; W_1, W_2 are liquid volumes supplied by high and low frequency generators to the HPH; W_0, dW is the initial fluid volume in the shells and its change; β is the coefficient of elasticity of the liquid в HPH; dp is the pressure drop in operating cavities; F_d is the driving force

Fig. 4. – Segment of structural diagrams of a hydrovolume vibration mechanism

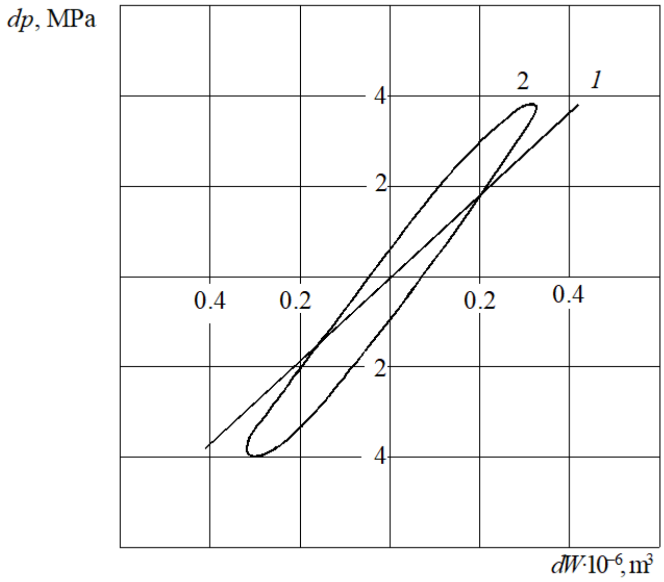

Fig 5. – Experimental characteristics of volumetric elasticity of HPH at W_1=0.44·10^{-6} m^3, p_0=4 MPa, ω_1=40 Hz

Other factors influencing the nonlinearity of the system are:

• variable initial pressure p_0;

• variable compression area of elastic shells S.

In the research [14], was shown a nonlinear relationship between the strain force of the HPH F and the amount of their deformation x. In this case, a typical dependency is subject to analysis:

$$F_{\mathrm{d}} = C_p(x) \cdot dx,$$

where F_{d} are the force transmitted through the HPH to the «ground», the driving force;

C_p is the hydraulic stiffness due to volumetric deformation;

dx – deformation of HPH.

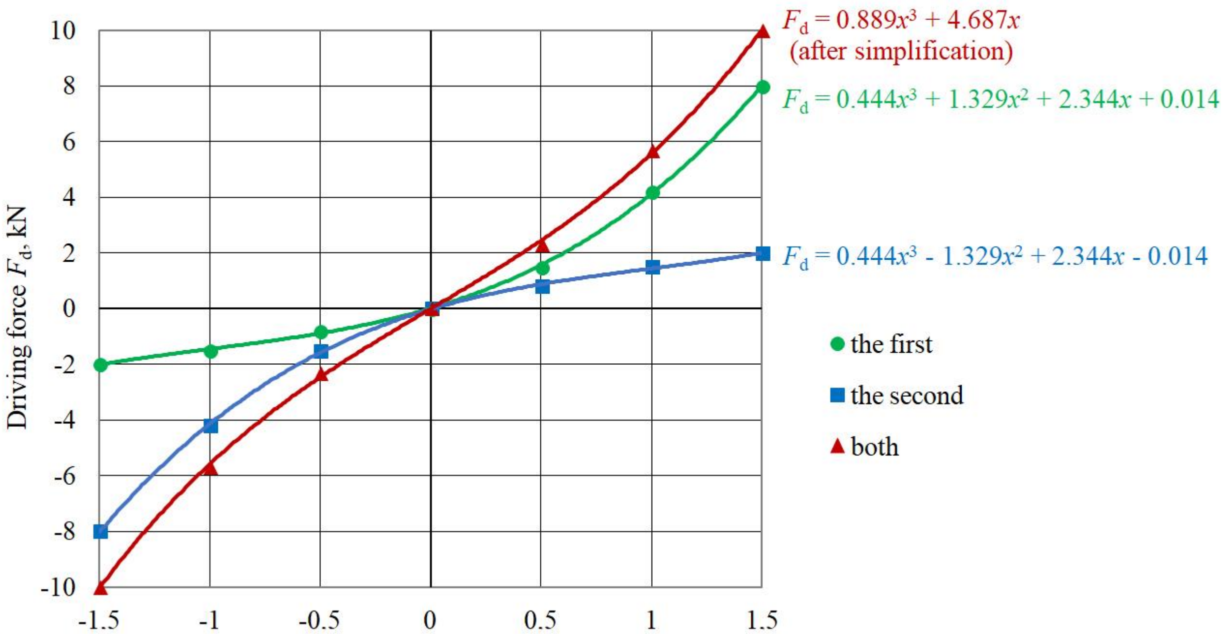

Fig 5. – Hydraulic stiffness of shells (polynomial approximation)

Thus, the system of equations (2) [15] can be rewritten as follows

$$dx = x_1' + x_2' - x;$$
$$F_d = C_p(x) \cdot \mathrm{d}x;$$
$$F_V = \alpha \cdot V;$$
$$F_x = C_0 \cdot x;$$

$$dF = F_d - F_V - F_x; \quad (2)$$
$$V(t) = \frac{1}{m}\int_0^t dFdt;$$
$$x(t) = \int_0^t dV(t)dt.$$

where α is the coefficient of viscous losses in the oscillatory circuit;

C_0 is the stiffness of the main elastic bonds;

dF, F_x, F_V are the force from the current deformation of the HPH, the force of the viscous internal resistance.

The final structural diagram of the hydrovolume vibration mechanism is shown in Figure 6 [23].

The non-constancy of the average pressure leads to a change in the stiffness of the shells C_p and the total stiffness of the system C_Σ. With an increase in the average pressure, the stiffness (slope of the characteristic) increases (Fig. 6) and the nonlinearity of the system decreases.

In this case, with separate excitation from each generator, symmetrical high-frequency and low-frequency, the link $C_p(x)$ is described by different equations:

$$F_{\text{d}} = 0.889 \cdot x^3 + 4.687 \cdot x \text{ (after simplification)}$$

and

$$F_{\text{d}} = 0.444 \cdot x^3 + 1.329 \cdot x^2 + 2.344 \cdot x.$$

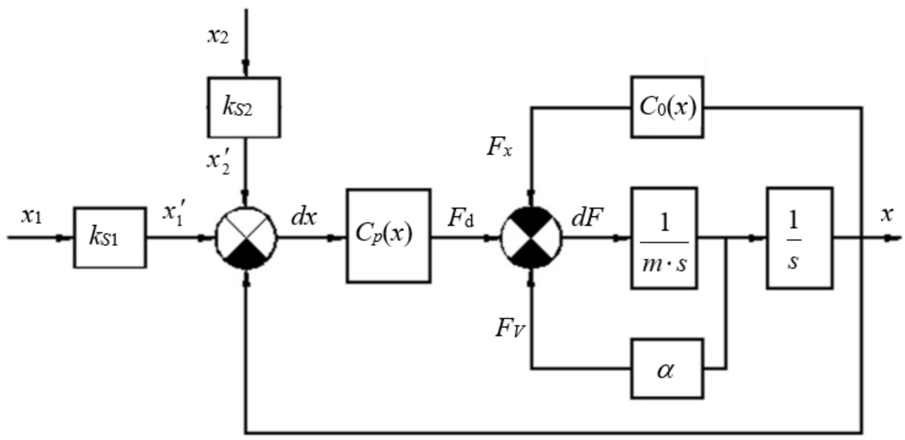

Fig 6. – Detailed structural diagram of a hydrovolume vibration mechanism with nonlinear connections

The presence of additional resonance can be explained by the fact that the system has at least three degrees of freedom, and not one along the vertical axis, designated and considered as the x coordinate (Fig. 7) [24,25].

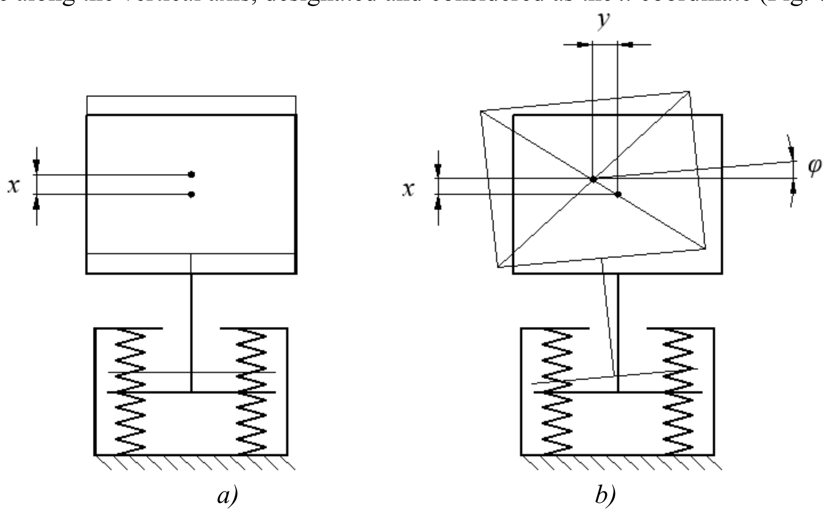

a) considered (with one degree of freedom); b) real (with three)

Fig 7. – Mechanical system of the vibration mechanism

Since during the oscillation process the energy of oscillations along the main coordinate x is pumped into the energy of oscillations along the coordinate y and φ [24]. In a real machine, which uses the energy of a load periodically falling in a certain guide housing, which has one degree of freedom in the vertical plane, there are no such phenomena. Therefore, side resonances are not considered in detail in this work.

Based on the experimental data obtained on the vibration stand, it is possible to:

• draw a conclusion about the degree of influence of a particular generator on the amplitude of the movement of the «output link» (Fig. 8);

• propose loading modes of the oscillatory system for further research into the possibility of exciting a combined signal with the simultaneous operation of two generators.

In this case, loading modes are understood as the ratio of the value of the input of one generator to the input of the other.

Based on the obtained equations, a system of equations was compiled:

$$\begin{cases} X_1 = 0.745 \cdot x + 0.179 \\ X_2 = 0{,}597 \cdot x + 0.185 \end{cases}.$$

The calculation carried out in the Mathcad program demonstrated the following result (Fig. 9): the generators load the oscillatory system (x=0.7 mm) almost equally with the input values X_1=0.603≈0.6 mm and X_2=0.701≈0.7 mm.

We accept the ratio of the inputs

$$\frac{X_1}{X_2} = \frac{0.6}{0.7}. \quad (1)$$

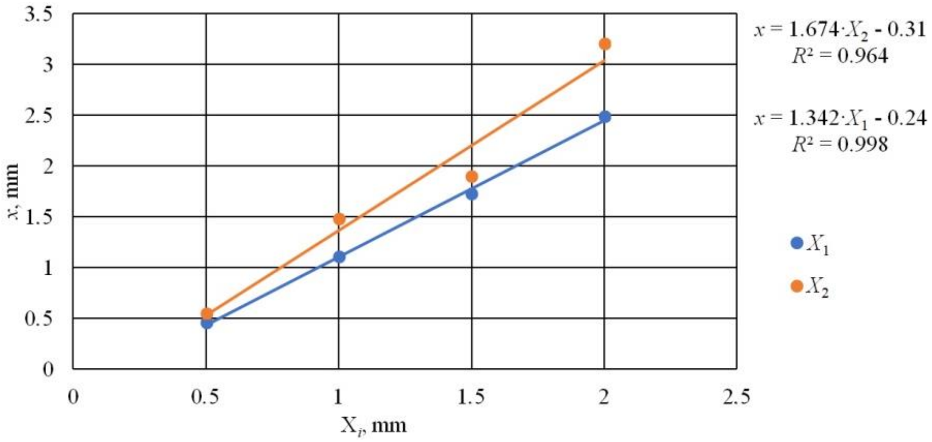

Fig. 8. – Dependence of the amplitude of the oscillation of the «output link» on the input X_1 and X_2

$x := 0, 0.1..1$

$X1(x) := 0.745 \cdot x + 0.179$

$X2(x) := 0.597 \cdot x + 0.185$

x =	$X1(x)$ =	$X2(x)$ =
0	0.179	0.185
0.1	0.254	0.245
0.2	0.328	0.304
0.3	0.403	0.364
0.4	0.477	0.424
0.5	0.551	0.484
0.6	0.626	0.543
0.7	0.701	0.603
0.8	0.775	0.663
0.9	0.849	0.722
1	0.924	0.782

Fig. 9. – Calculation results

Let us derive the relation (1) theoretically. The condition that determines the same disturbing effect on the movement of the "output link" x

$$W_1 = W_2$$

or

$$X_2 = X_1 \frac{S_1}{S_2}, \tag{2}$$

where S_1 is the working area of the high-frequency generator, which has four plungers with a diameter of d_1=7 mm.

Liquid is pumped into the HPH by two pistons:

$$S_1 = 2\frac{\pi \cdot d_1^2}{4} = 76.996 \text{ mm}^2, \tag{3}$$

where S_2 is the working area of the low-frequency generator with a plunger diameter d_2=9 mm

$$S_2 = \frac{\pi \cdot d_2^2}{4} = 63.617 \text{ mm}^2, \tag{4}$$

Based on the values of areas (3, 4), given the value X_1=0.6 mm, using formula (2) we obtain

$$X_{2\text{t}} = 0.6 \cdot \frac{76.97}{63.62} = 0{,}725 \text{ mm}, \tag{5}$$

The error will be

$$\Delta X_2 = \frac{X_{2\text{t}} - X_2}{X_{2\text{t}}} = \frac{0.725 - 0.7}{0.725} \cdot 100\% = 3.44 \text{ \%}. \tag{6}$$

From (6) we conclude that the experimentally found ratio X_1/X_2 (1) can be accepted for operation.

In further studies we will accept the loading modes (1:1, 1:2, 1:3):

$$\frac{X_1}{X_2} = \frac{1.2}{1.4} = \frac{1.2}{2.8} = \frac{1.2}{3.2}. \tag{7}$$

Conclusion

The working resonance frequency of the low-frequency generator has been found, which can be adjusted by changing the average pressure p_0.

With an increase in the average pressure, the stiffness of the system increases, thereby reducing its nonlinearity.

The system “responds” equally to the disturbing effect of one or another generator. There is insignificant difference in resonance frequencies and amplitude values of resonance peaks.

The presence of additional resonance at frequency ω_*'' is explained by several degrees of freedom of the mechanical system of the vibration mechanism.

It has been established that both generators can be adjusted to the same disturbing effect of the mechanical system.

References

[1] Akhmediev S.K., Filippova T.S., Oryntayeva G.Zh., Tazhenova G.D., Mikhailov V.F. Free and Forced Vibrations of the Carrier Beam of the Vehicle Chassis //Material and Mechanical Engineering Technology, 2023, Vol. 4. – P. 32-41. doi: 10.52209/2706-977X_2023_4_32.

[2] Kvon Sv.S., Kulikov V.Yu., Abylkairova M.M. Study of the Structure and Properties of 30CrMnNiMo Steel Subjected to Vibration and Heat Treatment // Material and Mechanical Engineering Technology, 2023, Vol. 2. – P. 3-9. doi: 10.52209/2706-977X_2023_2_3.

[3] Gavrilin A., Moyzes B., Zharkevich O. Constructive and processing methods of reducing vibration level of the metalworking machinery elements //Journal of Vibroengineering, 2015, Vol. 17, no 7. – P. 3495-3504

[4] Gavrilin A.N., Moyzes B.B., Kuvshinov K.A., Vedyashkin M.V., Surzhikova O.A. Determination of optimal milling modes by means of shock-vibration load reduction on tool and peak-factor equipment //Materials Science Forum, 2019, Vol. 942. – P. 87-96. doi: 10.4028/www.scientific.net/MSF.942.87.

[5] Sikhimbaev M.R., Sherov K.T., Zharkevich O.M., Sherov A.K., Tkachyova Y.O. Experimental studies of stabilization of boring cutter form – building top oscillation //Journal of Vibroengineering, 2012, Vol. 14, no 2. – P. 661-670.

[6] Plotnikova I., Vedyashkin M., Mustafina R., Plotnikov I., Tchaikovskaya O., Bastida J., Verpeta M. Optimization of the Stabilization System for Electromagnetic Suspension in Active Vibration Isolation Devices // MATEC Web of Conferences, 2016, Vol. 79. – 01019. https://doi.org/10.1051/matecconf/20167901019.

[7] Nizhegorodov A.I., Gavrilin A.N., Moyzes B.B., Kuvshinov K.A. Hydraulic drive of vibration stand for testing the robotic systems units by random vibration method // IOP Conference Series: Materials Science and Engineering, 2019, Vol. 516(1). – 012031. doi: 10.1088/1757-899X/516/1/012031

[8] Nizhegorodov A I, Gavrilin A N, Moyzes B B, Cherkasov A I, Zharkevich O M, Zhetessova G S, Savelyeva N A. Radial-piston pump for drive of test machines // IOP Conf. Series: Materials Science and Engineering, 2018, Vol. 289 (1). – 012014. doi:10.1088/1757-899X/289/1/012014.

[9]. Moyzes B., Gavrilin A., Kuvshinov K., Smyshlyaev A., Koksharova I. Using the Vibration Recorder Mobile Diagnostic Complex for Studying Vibration Processes //Material and Mechanical Engineering Technology, 2022, Vol. 3. – P. 50 – 57. doi: 10.52209/2706-977X_2022_3_50.
[10] Gavrilin A., Moyzes B., Cherkasov A., Mel′nov K., Zhang X. 2016 Mobile Complex for Rapid Diagnosis of the Technological System Elements //MATEC Web of Conferences, 2016, Vol. 79. – 01078 doi: 10.1051/matecconf/20167901078.
[11] Duan H., Zhu P., Peng S. Characteristic and processing method of SH-wave data generated by vibroseis source // Journal of Applied Geophysics, 2023, Vol. 214. – 105052. doi: https://doi.org/10.1016/j.jappgeo.2023.105052.
[12] Huang Zh., Shuai J., Hao L., et al. Investigation of radiative characteristics in the near field for shear, vertical and torsional vibroseis source //Soil Dynamics and Earthquake Engineering, 2024, Vol. 180. – 108628. doi: https://doi.org/10.1016/j.soildyn.2024.108628.
[13] Gao J., Xing X., Zhou X. Maximum deviation sliding search based stepped frequency synthesis method for marine vibroseis research //Measurement, 2022, Vol. 202. – 111799. doi: https://doi.org/10.1016/j.measurement.2022.111799.
[14] Moyzes B.B., Nizhegorodov A.I. The Study of the Parameters of Amplitude-Modulated Sweep Signal of the Shock Vibration Source of Seismic Signals // Engineering Materials, 2023, Part F1222. – P. 91-128. doi: https://doi.org/10.1007/978-3-031-38964-1_7.
[15] Moyzes B.B., Kuvshinov K.A., Nizhegorodov A.I., Vavilova G.V., Vtorushina A.N. The Study of the Dynamic Characteristics of the Hydro-volume Vibration Mechanism // Material and Mechanical Engineering Technology, 2024, Vol. 4. – P. 120-126. doi: 10.52209/2706-977X_2024_4_120.
[16] Lepetov V.A. Raschety i konstruirovanie rezino-tekhnicheskih izdelij [Calculations and construction of rubber products] / V.A. Lepetov, L.N. Yurcev. – Leningrad: Himiya, 1977. – 407 p.
[17] Lysenko E.N., Surzhikov A.P., Vlasov V.A. and et al. Synthesis of substituted lithium ferrites under the pulsed and continuous electron beam heating //Nuclear Instruments and Methods in Physics Research, Section B: Beam Interactions with Materials and Atoms, 2017, Vol. 392. – P.1-7.
[18] Lysenko E. N., Surzhikov A. P., Vlasov V. A. Malyshev A. V. and et al. Thermal analysis study of solid-phase synthesis of zinc- and titanium-substituted lithium ferrites from mechanically activated reagents Journal of Thermal Analysis and Calorimetry, 2015, № 3. – p. 1347-1353.
[19] Spivakovskij A.O. Vibracionnye konvejery, pitateli i vspomogatel'nye ustrojstva: nauchnoe izdanie [Vibrating conveyors, feeders and auxiliary devices: scientific publication] / A. O. Spivakovskij, I. F. Goncharevich. – Moscow: Mashinostroenie, 1972. – 327 p.
[20] Tarko L.M. Perekhodnye processy v gidravlicheskih mekhanizmah [Transients in hydraulic mechanisms] / L.M. Tarko. – Moscow: Mashinostroenie, 1973. – 167 p.
[21] Huang Zh., Xu H., Wang X., et al. Self-mixing interference signal analysis based on Lissajous figure convergence algorithm for vibration measurement //Measurement, 2024, Vol. 229. – 114407. doi: https://doi.org/10.1016/j.measurement.2024.114407.
[22] Zhang L., Xiao W., Fang W. A PGC demodulation scheme based on the Lissajous ellipse fitting for homodyne interferometer without using second harmonic carrier signal //Applied Acoustics, 2024, Vol. 221. – 109993. doi: https://doi.org/10.1016/j.apacoust.2024.109993.
[23] Moyzes B.B., Kuvshinov K.A., Nizhegorodov A.I., Vavilova G.V., Vtorushina A.N. //Material and Mechanical Engineering Technology, 2024, №4. – p. 120-126.
[24] Moyzes B.B., Krauin'sh P.Ya. Razrabotka vibroimpul'snogo mekhanizma s razdel'nym upravleniem vibracionnoj i impul'snoj sostavlyayushchimi [Development of a vibration pulse mechanism with separate control of vibration and pulse components] //Proceedings of the III Regional Scientific and practical Conference of students, postgraduates and young scientists "Modern technology and technology". – Tomsk: Publishing office ofTomsk Polytechnic University, 1997. – P.113-114.
[25] Prokop'ev V.N. Dinamika gidroprivoda [Hydraulic drive dynamics]. – M., Mashinostroenie, 1972 – 228 p.

Information of the authors

Moyzes Boris Borisovich, c.t.s., associate professor, National Research Tomsk Polytechnic University
e-mail: mbb@tpu.ru

Kuvshinov Kirill Aleksandrovich, senior lector, National Research Tomsk Polytechnic University
e-mail: kuvshinov@tpu.ru

Plotnikova Inna Vasilevna, c.t.s., associate professor, National Research Tomsk Polytechnic University
e-mail: inna@tpu.ru

Vavilova Galina Vasilevna, c.t.s., associate professor, National Research Tomsk Polytechnic University
e-mail: wgw@tpu.ru

Vtorushina Anna Nikolaevna, c.c.s., associate professor, National Research Tomsk Polytechnic University
e-mail: anl@tpu.ru